6. Fal'kovich G E, Shafarenko A B *Zh. Eksp. Teor. Fiz.* **94** 172 (1988) [*Sov. Phys. JETP* **67** 1393 (1988)]
7. Brazhnikov M Yu, Kolmakov G V, Levchenko A A *Zh. Eksp. Teor. Fiz.* **122** 521 (2002) [*JETP* **95** 447 (2002)]
8. Abdurakhimov L V, Brazhnikov M Yu, Levchenko A A *Pis'ma Zh. Eksp. Teor. Fiz.* **89** 139 (2009) [*JETP Lett.* **89** 120 (2009)]
9. Malkin V M *Zh. Eksp. Teor. Fiz.* **86** 1263 (1984) [*Sov. Phys. JETP* **59** 737 (1984)]
10. Ryzhenkova I V, Fal'kovich G E *Zh. Eksp. Teor. Fiz.* **98** 1931 (1990) [*Sov. Phys. JETP* **71** 1085 (1990)]
11. Kartashova E A *Physica D* **46** 43 (1990)
12. Kartashova E A *Physica D* **54** 125 (1991)
13. Pushkarev A N, Zakharov V E *Physica D* **135** 98 (2000)
14. Zakharov V E et al. *Pis'ma Zh. Eksp. Teor. Fiz.* **82** 544 (2005) [*JETP Lett.* **82** 487 (2005)]
15. Abdurakhimov L V, Brazhnikov M Yu, Remizov I A, Levchenko A A *Pis'ma Zh. Eksp. Teor. Fiz.* **91** 291 (2010) [*JETP Lett.* **9**1 271 (2010)]
16. Wright W B, Budakian R, Putterman S J *Phys. Rev. Lett.* **76** 4528 (1996)
17. Henry E, Alstrøm P, Levinsen M T *Europhys. Lett.* **52** 27 (2000)
18. Punzmann H, Shats M G, Xia H *Phys. Rev. Lett.* **103** 064502 (2009)
19. Brazhnikov M Yu, Kolmakov G V, Levchenko A A, Mezhov-Deglin L P *Europhys. Lett.* **58** 510 (2002)
20. Falcón C et al. *Europhys. Lett.* **86** 14002 (2009)
21. Westra M-T *Patterns and Weak Turbulence in Surface Waves* (Eindhoven: Technische Univ. Eindhoven, 2001)
22. Falcon É, Laroche C, Fauve S *Phys. Rev. Lett.* **98** 094503 (2007)
23. Kolmakov G V et al. *Prog. Low Temp. Phys.* **16** 305 (2009)
24. Brazhnikov M Yu, Levchenko A A, Mezhov-Deglin L P *Prib. Tekh. Eksp.* (6) 31 (2002) [*Instrum. Exp. Tech.* **45** 758 (2002)]
25. Abdurakhimov L V, Brazhnikov M Yu, Levchenko A A *Fiz. Nizk. Temp.* **35** 127 (2009) [*Low Temp. Phys.* **35** 95 (2009)
26. Abdurakhimov L V, Brazhnikov M Yu, Levchenko A A *J. Phys. Conf. Ser.* (2012), accepted
27. Kolmakov G V *Pis'ma Zh. Eksp. Teor. Fiz.* **83** 64 (2006) [*JETP Lett.* **83** 58 (2006)]
28. Donnelly R J, Barenghi C F *J. Phys. Chem. Ref. Data* **27** 1217 (1998)

PACS numbers: **95.75.–z**, **96.50.–e**, **96.60.–j**
DOI: 10.3367/UFNe.0182.201208j.0887

Motion of the Sun through the interstellar medium

V G Kurt, E N Mironova

1. Introduction

The motion of the Sun includes many components with different velocities, directions, and reference systems. For example, the Sun moves in a complicated open trajectory around the solar system barycenter. The maximum amplitude of this motion sometimes exceeds the radius of the Sun itself. This excursion is due to the motion of the most massive planets in the Solar System, Jupiter and Saturn, with the respective orbital periods 11.859 and 29.428 years. The Sun also moves relative to the 100 nearest stars in the direction toward the Hercules constellation with a velocity of 19.2 km s^{-1}. This motion was discovered by W Herschel (1738–1822) at the end of the 18th century based on the analysis of proper motions of the brightest (and correspondingly closest) stars. Naturally, Herschel could not express the value of this velocity in units such as km s^{-1} because he did not know the distance to these stars. Distances to stars were measured only in the early 1830s almost simultaneously by V Ya Struve (1793–1864) (Russia), F Bessel (1784–1846) (Prussia), and T Henderson (1798–1844) (England) using annual parallaxes of stars, which amount to only fractions of an arc second, even for the nearest stars. The direction to the apex of this motion is $\alpha = 270^\circ$ and $\delta = 30^\circ$.

The Sun also participates in an almost circular orbital motion around the galactic center with a velocity of 220 km s^{-1} in the direction perpendicular to the direction to the galactic center. With the distance 7.9 kpc to the galactic center, the orbital period of this motion is about 200 mln years, and during its life (5 billion years), the Sun has already made about 25 revolutions around the galactic center.

The Sun, together with the Galaxy, also has a peculiar velocity relative to nearby galaxies of the Local Group of galaxies. For example, the Galaxy approaches the center of the Andromeda nebula (M31) with a velocity of 290 km s^{-1} relative to the Solar System barycenter.

Finally, the Sun, together with the Milky Way and the Local Group, moves relative to the isotropic 3 K cosmic microwave background with the velocity (667 ± 22) km s^{-1} in the direction $l = 276^\circ \pm 3^\circ$ and $b = 30^\circ \pm 3^\circ$ (galactic coordinates). In a certain sense, this reference frame is a peculiar, singular coordinate system. Just this motion is responsible for the presence of the dipole component in the decomposition of cosmic microwave background in spherical functions. The amplitude of the dipole component is 6.706 mK.

This paper is focused on the study of the motion of the Sun relative to the local interstellar medium (LISM) on scales smaller than one or several parsecs but larger than 1000 astronomical units (a.u.).

2. Brief history of the discovery of the motion of the Sun relative to the local interstellar medium

In 1959, a group of astronomers from the Naval Research Laboratory (NRL) in the USA headed by G Fridman discovered a bright UV glowing of the sky from the rocket Aeroby-χ, which was capable of reaching only a 140 km altitude. The glow was measured in the atomic hydrogen line L_α ($\lambda = 1215.7$ Å) with the intensity reaching 20 kR (1 Rayleigh (R) = 10^6 photons cm^{-2} s^{-1} $(4\pi$ sr$)^{-1}$). The minimum of this glow was found to come from the anti-solar direction, and its intensity at a distance exceeding 90 km from Earth slowly decreased with increasing height [1]. In the same year, using a cell filled with molecular hydrogen supplied with a filament for its dissociation, which provided a sufficient amount of neutral hydrogen atoms for L_α line absorption, Morton determined that 7% of the discovered UV emission has a temperature exceeding 7000 K [2]. This could be explained by the presence of both a hot atomic hydrogen component in the upper atmosphere of Earth and an extra-atmosphere 'hot' emission component.

At almost the same time, starting in 1961, a research program of the Moon, Venus, and Mars explorations using automatic interplanetary stations (AISs) started in this country.

V G Kurt, E N Mironova Astro-Space Center, Lebedev Physics Institute, Russian Academy of Sciences, Moscow, Russian Federation
E-mail: vkurt@asc.rssi.ru

Uspekhi Fizicheskikh Nauk **182** (8) 887–894 (2012)
DOI: 10.3367/UFNr.0182.201208j.0887
Translated by K A Postnov; edited by A M Semikhatov

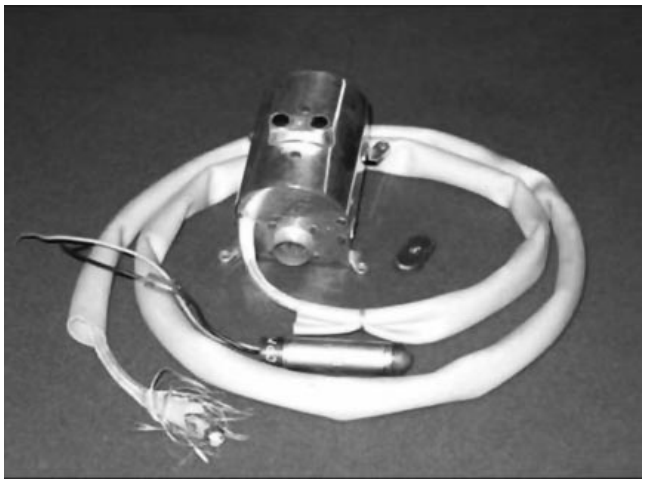

Figure 1. LA-2 two-channel ultraviolet (UV) photometer: the detector unit and Geiger counter.

In 1961, our group from the Sternberg Astronomical Institute of Moscow State University carried out similar studies of the upper atmosphere glow at altitudes up to 500 km using the R5 geophysical rocket. For this purpose, we constructed the two-channel ultraviolet photometer, LA-2 (Fig. 1), for observations in both the hydrogen L_α line and atomic oxygen triplet $\lambda = 1302, 1304$, and 1305 Å. A specially designed Geiger counter of photons filled with NO and an LiF or CaF_2 window with a diameter of 2 mm was used. From the shortwave side, the sensitivity of the detector was limited by the window transparency at $\lambda = 1050$ Å and $\lambda = 1225$ Å for LiF and CaF_2 respectively, while from the longwave side, the sensitivity of these detectors was limited by the ionization potential 9.3 eV ($\lambda = 1340$ Å) of nitrogen oxide. The first detector measured the total intensity in the L_α line and in the atomic oxygen triplet lines, while the detector with the CaF_2 window measured only the intensity of the atomic oxygen triplet lines.

Using the opportunity to install our detectors aboard the AIS launched to Venus and Mars, we were able to measure the extended hydrogen corona of Earth up to distances of 125,000 km, i.e., 20 Earth radii [3, 4]. To our surprise, at large distances (up to 100 mln km from Earth), the intensity did not vanish, but stayed almost constant at the level of 300–500 R, which, with the sensitivity of our detectors, corresponded to about 1000 counts per second. The counter with the calcium fluoride window allowed measuring the cosmic ray background, which was about 20–30 counts per second. Using the charged particle background suppression system enabled us to decrease this background rate to 2–3 counts per second. Theoretical estimates for the dependence of the interplanetary atomic hydrogen density on the solar wind particle flux and atomic hydrogen dissipation from the upper atmosphere of large planets could not explain such a high intensity of the neutral hydrogen atomic density in the interplanetary space. Nor could a detailed calculation of this emission intensity from even the nearest stars explain the observed effect, because the absorption by the interstellar dust and atoms with a low ionization potential (alkali metals) totally excluded the L_α line emission with such a high intensity. Scattering of solar L_α emission by the interstellar neutral hydrogen near the Sun was the only explanation for the effect observed. However, it was clear that an H II zone, similar to Stroemgren zones (a cavity filled with fully ionized hydrogen) found around hot early type O, B, and A giants, must exist around the Sun.

Calculations [5] showed that the observed intensity can be provided by the formation of an empty spherical region (cavern) around the Sun with a radius of 100 a.u. in an infinite medium (the Milne problem) filled with atomic hydrogen with a density of 0.01 cm^{-3}.

Indeed, exactly such zones of fully ionized hydrogen exist around hot blue early type (O, B, A) giants. The size of such a stationary Stroemgren zone is determined by the photon flux emitted by the star with $\lambda < 912$ Å and by the electron number density n_e of the medium. Equating the number of photons emitted by the star per second to the number of recombinations at all levels except the first one in the total volume of the Stroemgren sphere (the H II zone), we can calculate the Stroemgrem sphere radius

$$R_S = n_e^{-2/3}\left[\frac{4\pi F_*(L_c)(3/4)\,\pi}{\alpha_\Sigma - \alpha_1}\right]^{1/3},$$

where $4\pi F_*(L_c)$ is the total flux of quanta with the energy $h\nu > 13.56$ eV emitted by the star (L_c is the notation for the Lyman continuum), α_Σ is the recombination coefficient at all levels, and α_1 is the recombination coefficient at the first level.

The mass of gas confined inside the Stroemgren sphere exceeds that of the star itself by 100 or even 1000 times, and the radius of the Stroemgren sphere reaches several parsecs.

The boundary between the H II zone and the neutral-hydrogen zone H I is very thin (~ 0.05 pc), its width is $\Delta R_S = 1/n_H\sigma_i$, where n_H is the neutral hydrogen number density in the interstellar medium, of the order of 1 cm^{-3} and σ_i is the ionization cross section of atomic hydrogen near the ionization threshold, which is about 8×10^{-18} cm^2.

However, it is clear that the Stromgren theory is totally inapplicable to cold solar-type dwarf stars. Indeed, the time of ionization of a hydrogen atom at the distance 1 a.u. from the Sun is about 3×10^6 s, while the recombination time is 100–1000 times as long. Clearly, even with the velocity 10–30 km s^{-1} relative to the interstellar medium, the Sun 'flies' a distance of about 10^4 a.u. over the recombination time, forming a recombination tail 0.1 pc or even longer in size. This fact was first noted by theorists Blum and Far [6] from Bonn University.

Ionization of neutral hydrogen atoms passing by the Sun is in turn determined by two mechanisms: photoionization by hard emission from the solar corona with $h\nu > 13.56$ eV and charge exchange reactions with solar-wind protons. The effective cross section of the resonance charge exchange process of neutral hydrogen atoms with solar-wind protons is very high: at the maximum (close to 15 eV), it reaches 1.5×10^{-15} cm^2, and this process is 2–3 times more effective than photoionization.

Interstellar neutral hydrogen atoms, obviously, move in a hyperbolic trajectory, which is determined by the impact parameter P relative to the velocity at infinity V_∞. In polar coordinates, the trajectory is written as

$$\frac{1}{r} = \frac{GM_{\rm eff}(1+\cos\theta)}{V_\infty^2 P^2} + \frac{\sin\theta}{P},$$

where $M_{\rm eff} = M_\odot(1-\mu)$ and G is the gravitational constant. The factor $1-\mu$ takes the radiation pressure acting on a

hydrogen atom into account, which, as gravitation, is inversely proportional to the square of the distance from the Sun. This allows introducing the effective mass $M_{\rm eff}$ instead of the mass of the Sun, where μ is the ratio of the radiation pressure in the L_α line to the gravitational attraction force. At $\mu = 1$, hydrogen atoms move in straight trajectories. In this case, only ionization is effective.

The critical intensity in the L_α line center at which $\mu = 1$ is equal to 3.32×10^{11} photons per cm^2 per s. Such a high value of the intensity is hardly possible, even at the solar maximum activity. Nevertheless, the linear trajectory model is very convenient for approximate analytic calculations of the intensity of the observed scattered L_α radiation.

Next, to calculate the volume emissivity of the interstellar medium in the L_α line, we should include the Doppler shift from the projection of the hydrogen atom velocity in a hyperbolic orbit on the radius vector (centered in the Sun) of a point in the interplanetary space. Here, it is also necessary to take the complex profile of the L_α solar emission line with exponential wings into account. The total width of the L_α emission is about 1 Å, while the Doppler shift at the velocity about 30 km s^{-1} can reach 0.1 Å at a distance of the order of 1 a.u., which is quite substantial.

The probability that an atom flies without being ionized up to a point with polar coordinates r, θ is

$$p = \exp\left(-\frac{r_0^2\theta}{V_\infty \tau P}\right),$$

where $r_0 = 1$ a.u., V_∞ is the atom velocity 'at infinity', and τ is the lifetime, $1/\tau = 1/\tau_1 + 1/\tau_2$, where τ_1 and τ_2 are respectively the atom lifetimes at the 1 a.u. distance due to photoionization and charge exchange reactions with solar-wind protons.

Clearly, at each point of space, there are two types of atoms with different impact parameters P with the densities

$$n_1 = n_\infty \frac{(\sqrt{A}+1)^2}{4\sqrt{A}},$$

$$n_2 = n_\infty \frac{(\sqrt{A}-1)^2}{4\sqrt{A}},$$

where $A = 1 + 4M_{\rm eff}\, G/[V_\infty\, r\,(1+\cos\theta)\,]$.

It is clear that for $\mu = 1$, i.e., when gravitational attraction is fully compensated by radiation pressure acting on the hydrogen atom, $n_2 = 0$, which corresponds to the 'linear trajectory' model.

The volume emissivity $j(r,\lambda)$ [cm^{-3} 4π sr] can be written as

$$j(r,\lambda) = n(t,|\dot r|)\,\pi\Phi_{\rm S}(\lambda)\,p(\theta)\left(\frac{r_0}{r}\right)^2\sigma,$$

where $n(r,|\dot r|)$ is the atomic hydrogen density as a function of coordinates and the radial velocity, $\pi\Phi_{\rm S}(\lambda)$ is the solar radiation flux as a function of wavelength, and

$$p(\theta) = \frac{1}{16\pi}\left(\frac{11}{3} + \cos^2\theta\right)$$

is the scattering diagram.

To obtain the observed intensity, the volume emissivity should be integrated along the line of sight and over wavelengths within the solar L_α line width.

Such a primitive model assumes, clearly, that velocities of all atoms 'at infinity' are equal to V_∞ and are parallel to each other, which corresponds to zero temperature of the local interstellar medium. This model, called the 'cold model', can be applied with sufficient accuracy only in the region ahead of the solar motion direction in the LISM within the angle $\theta_{\rm cr} = \arctan(V_{\rm T}/V_\infty)$, which approximately corresponds to $\theta = 27°$, where $V_{\rm T}$ is the thermal velocity of atoms, which is equal to $\sqrt{2kT/m_{\rm p}}$. For larger angles, the Maxwellian distribution of hydrogen atoms over both velocity modulus and direction must be taken into account. For this, we should integrate 'cold models' with a weight proportional to the Maxwellian velocity distribution and homogeneous distribution over angles.

Therefore, to tune the 'cold model' to the observational data, the following parameters of the Sun motion in the LISM should be determined:

V_∞, the absolute value of the Sun's velocity;

λ and β, the two angles characterizing the direction of the Sun's motion in the ecliptic coordinates, which can then be easily transformed into the galactic coordinates;

n_∞, the hydrogen atom number density at infinity;

μ, the ratio of the radiation pressure force to the gravitational attraction force;

$\pi\Phi(0)$, the intensity in the solar emission L_α line center;

T_∞, the temperature of hydrogen atoms at infinity.

Hence, the minimum number of sought parameters is 7. However, the agreement between theory and observations can be improved by introducing additional parameters, for example, the solar proton flux anisotropy as a function of the heliographic altitude, because the charge exchange process dominates in the ionization of hydrogen atoms.

Figure 2 shows the distribution of the L_α volume emissivity inside the Solar System.

In [7], using the 'hot model', an analytic expression for the helium atom density along the Sun's direction of motion was also obtained, which allows 'sewing' the data on the helium atom number density ahead of the Sun's motion to that in other directions and thus obtaining the complete picture of

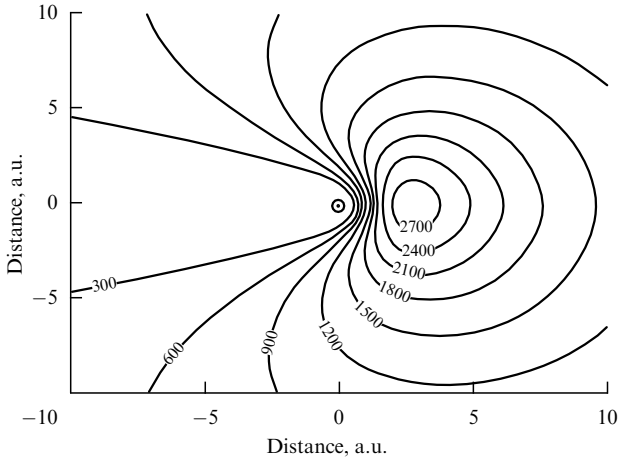

Figure 2. The volume L_α-line luminosity distribution [cm^{-3} s^{-1}] for the model parameters $V_\infty = 20$ km s^{-1}, $\tau = 1.2 \times 10^6$ s, and $\mu = 1$. The plane of the figure represents one of the cuts passing through the direction of the wind and the Sun. The upwind direction is to the right. The region with the maximum volume luminosity is located between 2 a.u. and 4 a.u. in the upwind direction.

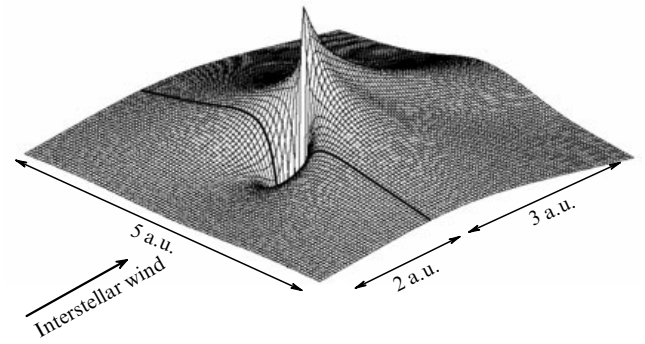

Figure 3. The volume luminosity in the He I $\lambda = 584$ Å line in the plane passing through the Sun and the wind axis (for the model parameters $V_\infty = 25.5$ km s^{-1}, $T = 7000$ K, and $\tau = 1.0 \times 10^7$ s, the Doppler width of the solar $\lambda = 584$ Å line is $W_D = 35.5$ km s^{-1}). Solar parameters are assumed to be isotropic.

the atom number density inside the Solar System. Figure 3 shows the atomic helium density at distances up to 10 a.u. [8]. The sharp minimum (about 0.3 a.u.) is due to photoionization of helium atoms near the Sun.

In addition, it is necessary, although it is unclear how, to account for the interaction of hydrogen atoms with the high-temperature plasma between two shocks (probably supersonic) that were formed by solar wind stopping at a distance of about 100 a.u. and by interstellar medium stopping at a distance of 200 a.u. Clearly, this effect is not dominant, because the effective conventional 'optical depth' for number densities about 10^{-3} or 10^{-4} cm^{-3}, the cross section less than 10^{-15} cm^2, and the length of the intermediate zone between the LISM and the heliosphere about 10^{15} cm does not exceed 10^{-3} or 10^{-2}. Nevertheless, this question remains open (see [9, 10]) and its solution can possibly slightly change the LISM parameters discussed below.

An important question is the determination of the profile of scattered radiation in the L_α line, which would allow an independent measurement of the incident interstellar matter flow. However, to solve this problem, an optical dispersion or interferometric spectrometer is needed, which is not an easy task for the radiation intensity of only 500 R at the maximum and the line width less than 0.1 Å. To solve this problem, very much as R Wood did in his experiments with sodium vapors, we used an absorbing cell filled with atomic hydrogen, similar to what was used by Morton in the first rocket observations of the L_α-emission.

Clearly, the observed bolometric intensity after passing through the cell filled with atomic hydrogen can be written as

$$I(\tau_0, T_E, T_A) = I(0)\,\frac{1}{\pi}\int_0^\infty \exp\left\{-x^2 - \tau_0 \exp\left[-\frac{T_E}{T_A}\left(x - \frac{V_r}{c}\right)\right]^2\right\} dx,$$

where τ_0 is the optical depth of the cell in the L_α line center, T_E and T_A are the respective radiation temperatures of the LIMS and atomic hydrogen in the cell, V_r is the radial velocity component of a hydrogen atom, and c is the speed of light in the vacuum. As the first approximation, we used the Doppler profile of the LISM emission line. The cell temperature (close to 300 K) was measured by a temperature probe on the cell surface. For the ratio $T_E/T_A \gg 1$ and $\tau_0 = 10$, the approximate expression:

$$RF = \frac{I}{I_0} = 1 - \frac{32.2}{\sqrt{T_E}} \exp\left(-\frac{60.6 V_r^2}{T_E}\right),$$

is valid for $T_E = 7000$ K with an accuracy better than 5%.

A more precise expression, taking both the L_α- absorption and scattering inside the cell into account, was obtained in [11].

3. Observations and data processing

Observations of the intensity of scattered L_α-radiation by a diffraction spectrometer and photometers both with and without an absorbing cell filled with hydrogen were carried out by us from the Venera and Mars IASs. However, the best observations were apparently obtained in the joint Soviet–French experiments aboard the Prognoz-5 and Prognoz-6 satellites (Fig. 4). Both satellites moved in highly eccentric orbits with an apogee of about 200,000 km, a perigee of about 1000 km, and an orbital period of 4 days. The principal inertia moment axes of the satellites were pointed toward the Sun, and the satellites rotated around them with a spin period of 2 min, corresponding to the angular velocity 3 deg s^{-1}. During the axial rotation, special optical trackers periodically registered Earth, the Moon, and the Sun passing across their field of view, which allowed calculating the Euler angles and extrapolating the orientation of the satellites for the subsequent 12 h interval of time. Then, new rotation parameters were determined. The reorientation of the main inertia axis to the Sun was repeated every 4–10 days. The correctness of the orientation was checked by matching the results at the beginning of the next 12 h interval. The system of orientation of the apparatus axes was controlled by observing hot bright stars with a UV photometer. Using this method, the orientation of the optical axis of the photometer was determined with an accuracy of 1–2 deg, and sometimes better. The photometers had two optical axes; the main one

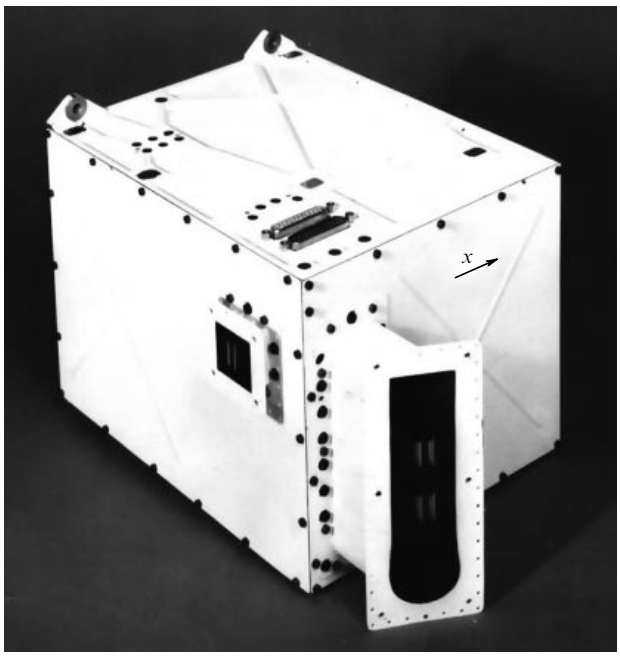

Figure 4. General view of the four-channel UV photometer installed aboard the Prognoz-5 and Prognoz-6 satellites.

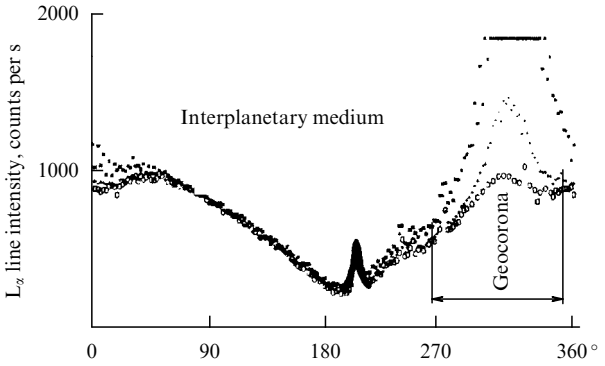

Figure 5. The L_α-line intensity distribution for three scan circles corresponding to three positions of the satellite in orbit. The narrow peak is a hot star, wide maxima near 310 deg are due to the geocorona. The signal between 50 and 150 deg is due to the interplanetary L_α-line emission.

had three detectors centered on the H I L_α line and the He I ($\lambda = 584$ Å) and He II ($\lambda = 304$ Å) lines supplied with the absorbing cell and a narrow-band interferometric filter in the L_α-channel. For the He I and He II channels, broadband filters made of thin metal films with a bandwidth of 100 Å were used. The optical axes of these channels were directed normally to the spin axis of the satellite, i.e., normally to the direction to the Sun. An additional He I channel was oriented at an angle of 10 deg to the anti-solar direction. The Prognoz-5 and Prognoz-6 satellites actively operated for four and six months, respectively. The telemetry was received once every 10.7 s, but because the spin period of the satellite (120 s) and the time the telemetry was taken were incommensurable, the intensity and reduction factor (the ratio of switched-on to switched-off cells of the H I L_α-detector) depended on the spin angle of the satellite continuously with a high spatial resolution (about 1–3 deg). Clearly, all scan trajectories passed through both ecliptic poles, which provided constant control of the detector sensitivity stability. Figures 5 and 6 show examples of scans in the H I L_α line and FR. The passage of the field of view through Earth's hydrogen corona is clearly seen.

In the data processing, all points with the impact parameter of the optical axis passed at distances smaller than 50000 km for the L_α line and 70000 for the He I ($\lambda = 584$ Å) line were rejected. This excluded the influence of extended hydrogen and helium atmospheres of Earth. The He II ($\lambda = 304$ Å) channel was used by us as the 'background' channel registering cosmic rays and induced radiation from the spacecraft. Its counts were subtracted from those of all other detectors. We note that in the H I L_α channel, the count rate was 100 times higher than in the He I ($\lambda = 584$ Å) channel. Figure 7 clearly demonstrates how the optical axis of the detector crosses the focusing cone of helium atoms 'behind the Sun'.

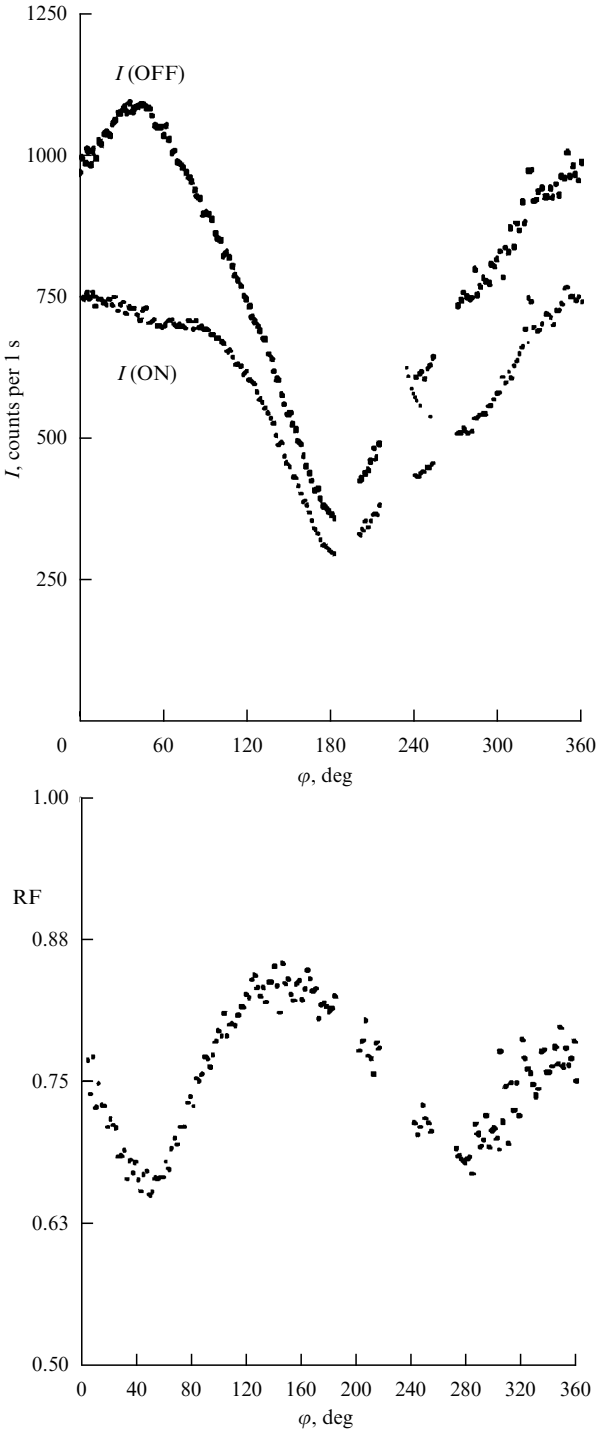

Figure 6. Observed intensity of the L_α line along the scan circle with a turned-on, I(ON), and turned-off, I(OFF), cell. The reduction factor is RF = I(ON)/I(OFF).

4. Measurement of LISM parameters

When interpreting H I observations, all data were fitted to obtain all LISM parameters simultaneously [12]. In exactly the same way, the French group processed the He I results [13]. Our group divided all parameters into two parts. The solar data (the He I line width and the lifetime of a helium atom at a distance of 1 a.u.) were taken from the literature. The direction of the Sun's motion in the LISM (two angles in the ecliptic coordinate system) was determined from the easily observed maximum of the glow on the He I ($\lambda = 584$ Å) line, i.e., when the optical axis of the detector crossed the focusing cone axis. Two parameters were fitted: the LISM temperature and the absolute value of the Sun's velocity [14–16]. In our opinion, the fitting with only two parameters gives more reliable results than fitting with a larger number of parameters. We note that the determination error of the Sun's velocity relative to the LISM does not exceed 2 km s^{-1}, while the temperature is determined with a much worse accuracy.

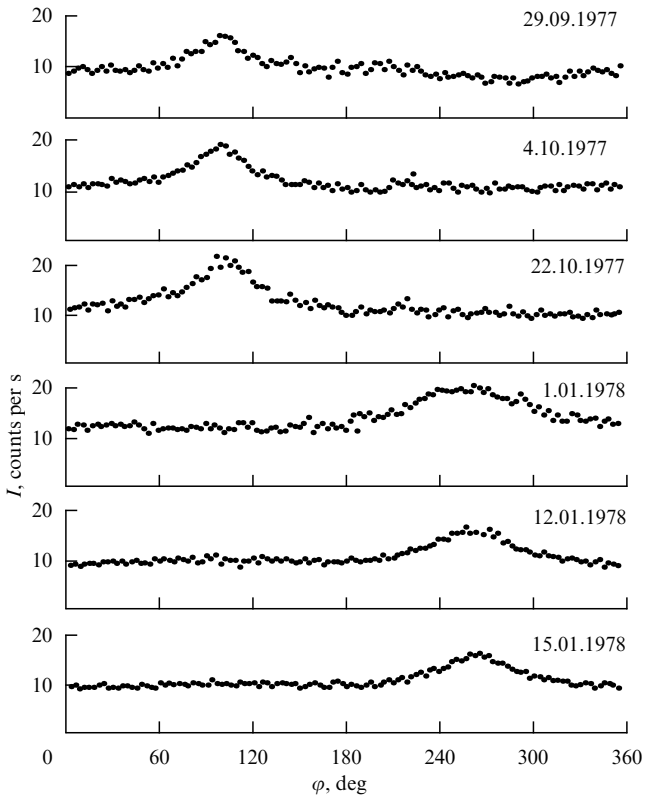

Figure 7. The He I ($\lambda = 584$ Å) line emission intensity along six scan circles during the passage through the maximum helium atom density cone.

Tables 1 and 2 list the results obtained by us and from measurements by the EUVE (Extreme Ultraviolet Explorer) and SOHO/SWAN (Solar and Heliospheric Observatory/ Solar Wind Anisotropy) satellites. The coordinates of the downwind direction measured by the Prognoz-5 and Prognoz-6 satellites are related to the epoch 1950,0, while those measured by the EUVE and SOHO satellites, to the epoch 2000,0.

Both hydrogen and helium densities are factors in the expression for the observed intensity. Clearly, their determination accuracy depends only on the absolute calibration of the detectors, i.e., on the recalculation of the observed count rate into physical units erg cm^{-2} s^{-1} sr^{-1} or Rayleighs. For calibration, we used two sources whose intensity can be calculated based on several parameters; for a blackbody (BB) source, only one parameter (its temperature) is needed. However, for our observations in the vacuum UV range, a source with a temperature of 10,000 K are even 20,000 K was required. Such sources were manufactured by us jointly with the Institute of High Temperatures, RAS using high-pressure lamps filled with gas (for example, xenon). However, determination of the temperature with the required accuracy (about 25 K) is a very complicated problem. Obviously, the black-body approximation can be used only in lines, because in the continuum, the hot gas emission is optically thin and the black-body formula cannot be applied. The radiation is optically thick and corresponds to the black-body intensity only in the emission lines. We used the method of the Balmer line width determination for hydrogen, which was added to the noble gas in small amounts (1–3%). This allowed estimating the electron density in the lamp, which, in turn, is determined by the Saha formula, and thus the temperature was ultimately calculated. Unfortunately, the absolute calibration accuracy obtained by this method was rather low (more than 50%) due to errors in the temperature determination. In addition, it proved to be very difficult to take a huge radial temperature gradient in the gas-discharge tube into account, with the temperature changing from 25,000 K on the tube axis to 300 K on the fresh-water-cooled walls.

Synchrotron radiation is the second source with the known absolute intensity. To calculate its intensity, the curvature radius of the relativistic electron trajectory, magnetic field strength, energy of the electron, and the number of electrons in the accelerator channel should be known. We used the VEPP-2M electron–positron accelerator of the Nuclear Physics Institute, Siberian Branch of RAS, where our group was invited by A M Budker, who was the director of the institute at that time. Using this method allowed increasing the absolute calibration accuracy to 15–20%. Finally, during the satellite flight, we could test or improve the calibration by observing bright blue and hot stars accidentally occurring in the field of view of the detectors.

5. Direct (nonoptical) methods of measurements of the local interstellar medium parameters

As far as we know, the first successful measurements of the atomic helium density were carried out by a group of researchers from the Max-Planck Institute for Aeronomy (Lindau, Germany) using detectors aboard the Ulysses extra-ecliptic station of the European Space Agency, launched on 6 October 1990 and operated until 1 July 2008, i.e., for 17 years [17]. Ulysses crossed the ecliptic

Table 1. LISM parameters from Prognoz 5, 6 observations of the He I ($\lambda = 584$ Å) line.

Satellite	$\lvert V\rvert$, km s^{-1}	λ, deg	β, deg	T, K	n (He I), cm^{-3}
Prognoz-6 (our results [12])	25.3 ± 1.9	77.5 ± 2.6	-6.2 ± 2.1	$13{,}500 \pm 1700$	0.018 ± 0.002
Prognoz-5 (results of the French group [13])	27 ± 3	74.5 ± 3	-6 ± 3	11,000 – 24000	0.015 ± 0.0023
EUVE (USA)	24.5	74.7 ± 0.5	-5 ± 0.1	7000	0.0135 ± 0.08

Table 2. LISM parameters from Prognoz 5, 6 observations of the L_α line.

Satellite	$\lvert V\rvert$, km s^{-1}	λ, deg	β, deg	T, K	n (H), cm^{-3}
Prognoz-5 and Prognoz-6	20 ± 1	71 ± 2	-7.5 ± 3	8000 ± 1000	0.065 ± 0.015
SOHO (SWAN)	21.5 ± 0.5	72.3 ± 0.7	-8.7 ± 0.9	$11{,}500 \pm 500$	?

Table 3. LISM parameters from the Ulysses measurements of the helium atom flux.

$\lvert V\rvert$, km s^{-1}	λ, deg	β, deg	T, K
26 ± 1	72 ± 2	-2.5 ± 2.7	6700 ± 1500

plane four times and could observe both solar poles. In particular, the latitude asymmetry of the solar wind was measured, which directly confirmed our results obtained from the Prognoz satellites [18].

To register helium atoms that entered the Solar System from the interstellar medium, a group of researchers headed by H Rosenbauer at the Max-Planck Institute for Aeronomy designed a detector based on the interaction of helium atoms having an energy of about 15 eV (which corresponds to the velocity of 25 km s^{-1}) with a thin gold foil. Electrons kicked out from the foil were detected by a channel photomultiplier, which, with the known velocity of the electrons, allowed estimating their local density (in contrast, in our integral method, the radiation on the $\lambda = 584$ Å line was measured along the entire path from the measurement point to infinity). The detector scanned almost the entire sky, enabling the determination of the direction of helium atom trajectories. The measurements were carried out from different points in the Solar System, owing to which a high accuracy was achieved (Table 3). Data obtained in a completely different way are in good agreement with our results obtained by 'optical' means.

6. Conclusion

From the brief consideration of the problem of the motion of the Sun relative to the local interstellar medium given above, we conclude that the basic parameters of the LISM are known quite well. These include the density of atomic hydrogen and helium in the close vicinity of the Solar System (at distances exceeding 20 a.u.) and the direction of the motion of the Sun relative to LISM. The LISM temperature is known with less accuracy. Undoubtedly, the temperature values derived by us from measurements on L_α lines of hydrogen ($\lambda = 1215.7$ Å) and helium ($\lambda = 584$ Å) are different, and this fact calls for explanation. Second, the temperature measurement error on these two lines highly exceeds the relative measurement errors of the solar motion direction relative to the LISM and of the hydrogen and helium atomic density.

It is very plausible that the temperature difference for hydrogen and helium atoms is due to the interstellar atoms crossing the transient zone between the heliosphere and 'pure' interstellar space. Hopefully, new results obtained by the IBEX (Interstellar Boundary Explorer) satellite can be used to improve the parameters of the local interstellar medium.

References

1. Kupperian J E (Jr.) et al. *Planet. Space Sci.* **1** 3 (1959)
2. Morton D C, Purcell J D *Planet. Space Sci.* **9** 455 (1962)
3. Bertaux J L et al. *Kosmich. Issled.* **16** 269 (1978) [*Cosmic Res.* **16** 214 (1978)]
4. Bertaux J L et al. *Astron. Asrophys.* **46** 19 (1976)
5. Kurt V G, Germogenova T A *Astron. Zh.* **44** 352 (1967) [*Sov. Astron.* **11** 278 (1967)]
6. Blum P W, Fahr H J *Astron. Astrophys.* **4** 280 (1970)
7. Blum P W, Pfleiderer J, Wulf-Mathies C *Planet. Space Sci.* **23** 93 (1975)
8. Lallement R et al. *Astron. Astrophys.* **426** 875 (2004)
9. Baranov V B *Space Sci. Rev.* **143** 449 (2009)
10. Katushkina O A, Izmodenov V V *Pis'ma Astron. Zh.* **36** 310 (2010) [*Astron. Lett.* **36** 297 (2010)]
11. Bertaux J L, Lallement R *Astron. Astrophys.* **140** 230 (1984)
12. Bertaux J L, Lallement R, Kurt V G, Mironova E N *Astron. Astrophys.* **150** 1 (1985)
13. Dalaudier F, Bertaux J L, Kurt V G, Mironova E N *Astron. Astrophys.* **134** 171 (1984)
14. Burgin M S et al. *Kosmich. Issled.* **21** 83 (1983) [*Cosmic Res.* **21** 72 (1983)]
15. Kurt V G, Mironova E N, Bertaux I L, Dalaudier F *Kosmich. Issled.* **22** 97 (1984) [*Cosmic Res.* **22** 86 (1984)]
16. Kurt V G, Mironova E N, Bertaux J L, Dalaudier F *Kosmich. Issled.* **22** 225 (1984)
17. Witte M et al. *Adv. Space Res.* **13** (6) 121 (1993)
18. Lallement R, Bertaux J L, Kurt V G *J. Geophys. Res.* **90** 1413 (1985)

PACS numbers: **04.20.–q**, **04.70.–s**, **98.80.–k**
DOI: 10.3367/UFNe.0182.201208k.0894

Generation of cosmological flows in general relativity

V N Lukash, E V Mikheeva, V N Strokov

1. Introduction

The Copernicus principle is known to cast doubt on the uniqueness of our Universe. Therefore, it seems likely that there is some physical mechanism of gravitational reproduction of cosmological flows of matter expanding from super-large to small curvatures and densities. We relate the solution of the cosmogenesis problem (the origin of universes) to black holes, in which regions with high space–time curvature are formed in a natural evolutionary manner during gravitational collapse. We only need to continue the singular states that appeared in this way in time and to see what geometrical structures are found beyond them in the future.

An analytic continuation of general relativity (GR) solutions through singular hypersurfaces $r = 0$ is realized in the model class of 'black-white' holes with integrable singularities [1, 2]. In these models, the space–time of a black hole can be connected with a white hole endowed with the metric of a homogeneous cosmological model, allowing an explicit realization of the geometrical concept of a multisheet universe (hyperverse). These topics are discussed in this paper.

2. How the Schwarzschild metric can be continued

A black hole with a positive external mass $M > 0$ without rotation or charge is described in GR by the Schwarzschild metric in the vacuum:

$$\mathrm{d}s^2 = \left(1 - \frac{2GM}{r}\right)\mathrm{d}t^2 - \frac{\mathrm{d}r^2}{1 - 2GM/r} - r^2\left(\mathrm{d}\theta^2 + \sin^2\theta\,\mathrm{d}\varphi^2\right), \quad (1)$$

V N Lukash, E V Mikheeva, V N Strokov Astro-Space Center, Lebedev Physics Institute, Russian Academy of Sciences, Moscow, Russian Federation
E-mail: lukash@asc.rssi.ru, helen@asc.rssi.ru, strokov@asc.rssi.ru

Uspekhi Fizicheskikh Nauk **182** (8) 894 – 900 (2012)
DOI: 10.3367/UFNr.0182.201208k.0894
Translated by K A Postnov; edited by A M Semikhatov